

Some Issues of Rough Surface Contact Plasticity at Micro- and Nano-Scales

Y. F. Gao, A. F. Bower and K.-S. Kim
Division of Engineering,
Brown University,
Providence, RI 02912, U.S.A.

ABSTRACT

Rough surface contact plasticity at microscale and nanoscale is of crucial importance in many new applications and technologies, such as nano-imprinting and nano-welding. This paper summarizes our recent progress in understanding contact plasticity from a multiscale point of view, and also presents our perspectives. We first discuss a contact model based on fractal roughness and continuum plasticity theory. Interestingly, our simple, elastic-plastic contact model of the Weierstrass-Archard type gives rise to many practical scaling relations of contact pressure, contact compliance etc. The usefulness of those predictions is discussed for experimental measurements of the thermal/electrical contact resistance. A material length scale can be introduced by a nonlocal plasticity theory, or implicitly by dislocation mechanics modeling. The recent work on micro-plasticity of surface steps gives a variety of surface yielding and hardening behaviors, depending on interface adhesion, roughness features and slip systems. As a consequence, a rough surface contact at mesoscale can lead to the formation of a boundary layer with sub-layer dislocation structures, which cannot be predicted by existing strain gradient plasticity theories. The micromechanical analysis of surface plasticity could serve as the connection between microscale bulk dislocation plasticity and nanoscale atomistic simulations.

INTRODUCTION

Many important mechanical properties and failure problems are governed by rough surface contact at microscale and nanoscale. Recent technological advancements, such as nanoscale imprinting and cold-welding [1], require fundamental understandings of rough surface contact plasticity, adhesion and friction at small length scales. Rough surface contact plasticity is intrinsically a multiscale problem because of the multiscale nature of surface roughness, the structure- and size-sensitive material deformation behavior, and the importance of surface forces and other physical interactions. The surface roughness is usually characterized by the power spectral density function (PSDF), which is the Fourier transform of the spatial autocorrelation function of the roughness profile. For an ideally self-affine fractal surface, the PSDF is a straight line and the slope tells the fractal dimension. A real rough surface might be piece-wise fractal (i.e. different fractal dimensions at different scale ranges), or not fractal at all. For example, a cleaved surface of LiF is very flat elsewhere except some widely separated surface steps.

For large scale contacts, even if we restrict our attention to the use of classic plasticity theory, there is no agreement on the prediction of contact pressure distribution, contact compliance and other properties [2,3]. Motivated by the recent work in [4], we have carried out an elastic-plastic contact analysis of a fractal rough surface, which is idealized with a Weierstrass series. Scaling relations of the total contact area versus the applied load and roughness properties can be deduced [5], and compared with numerical simulations that have pre-specified spatial

cutoff sizes [6,7]. We also discuss the validity conditions of predictions that are based on contact compliance, such as thermal/electrical contact resistance [8-10].

At microscale and nanoscale, it is worth noting that we still lack sufficient incorporation of micromechanics and novel deformation mechanisms. A material length scale can be introduced by simply using the Nix-Gao strain gradient plasticity [11], which leads to the conclusion that small asperities tend to deform elastically for an ideally fractal surface contact [12]. Many present dislocation plasticity studies are based on bulk sources and reactions [13,14]. For mesoscale multiple asperity contacts, surface roughness can be sources and sinks of dislocations. The study of cooperative behaviors of defects and the interaction with rough surfaces is the subject of surface micro-plasticity. Even though the roughness is usually confined to a very thin layer, the resultant dislocations can extend to a far depth. This type of discrete-dislocation analysis with surface sources provides the connection between atomistic simulations and the slip-line analysis that is based on a continuous dislocation distribution density. We will discuss some of our latest works along this line [15,16], and possible connections with atomistic simulations [15,17].

SCALING RELATIONS FROM IDEALLY FRACTAL SURFACE CONTACT

The following analysis only considers the classic continuum plasticity. Following Ciavarella et al. [4], we study the elastic-plastic contact of an ideally fractal rough surface by a model of the Weierstrass-Archard type. A fractal rough surface can be idealized by the Weierstrass series,

$$z(x) = A_0 \sum_{n=0}^{\infty} \gamma^{(D-2)n} \cos(2\pi\gamma^n x / \lambda_0),$$

where A_0 and λ_0 are amplitude and period of the longest wave, D is the fractal dimension ($1 < D < 2$), and γ is a fitting parameter (usually taken to be 1.5). We proceed from contacts at coarse scales, and compute the evolution of contact pressure distribution as more roughness details are included as specified in the Weierstrass series. The nominally flat surface contact at the $(n-1)$ -th scale is supported by many small asperities at the n -th scale, as shown in Fig. 1(a). The link between two successive scales is by the assumption that the nominal pressure at the fine scale is equal to the true pressure at the coarse scale. Therefore, if we know the initial pressure and the roughness information, we can compute the contact area, pressure, compliance, contact size distribution and many other contact properties. We further assume the asperity contact pressure be uniform, which significantly simplifies our calculations in contrast to the exact calculations in [4]. It is worth noting that the Archard's pressure relation is only justified when the two successive scales have large difference in contact stiffness. This is usually true if the two successive scales are far apart; otherwise, we need to devise a nonlinear coupling scheme, for example, by the elastic foundation model. A comparison of those methods and the modeling details can be found in [5].

The normalized applied pressure is $\tilde{p} = F / \pi E^* A_0$ with the applied load F (per unit length in the out-of-plane direction) and the composite modulus E^* . We define $\psi_n = E^* A_n / \sigma_Y \lambda_n$ (and therefore $\psi_n = \psi_0 \gamma^{(D-1)n}$ with $\psi_0 = E^* A_0 / \sigma_Y \lambda_0$), where σ_Y is the yield stress, and A_n and λ_n are amplitude and period of the n -th scale. For an ideally fractal surface, ψ_n increases to infinity because $\gamma > 1$ and $1 < D < 2$. This is also related to the observation that the rms asperity slope goes up to infinity with increasing asperity measurement resolution. Three asymptotic analyses are presented next. For an elastic fractal surface, with more and more roughness details included,

the contact will be supported by infinite number of zero-size contacts, and each of them has infinite pressure [4]. The total true contact area, L_n at the n -th scale, is given by

$L_n/\lambda_0 \approx 0.4\gamma^{-(D-1)(n-1)}\tilde{p}$, as depicted by the rapidly decreasing line in Fig. 1(b). The work in [5]

studies the rigid-perfectly plastic material. If the lateral interaction between plastic deformations of neighboring asperities is weak, the contact area is simply given by the load divided by the hardness, i.e. $L_n/\lambda_0 = F/\lambda_0 H$ with material hardness $H \approx 3\sigma_Y$. This asymptotic solution is shown by the line with circles in Fig. 1(b). With strong interference between adjacent asperities, the plastic deformation of one asperity is constrained by its neighbors, and the contact pressure can rise up to a value twice the material hardness. This type of pressure rise-up and lateral constraints are also discussed in §13.2 of [3]. The asymptotic solution is given by

$L_{n \rightarrow \infty}/\lambda_0 = F/\lambda_0 H^*$ with $H^* \approx 6\sigma_Y$, as shown by the line with squares in Fig. 1(b).

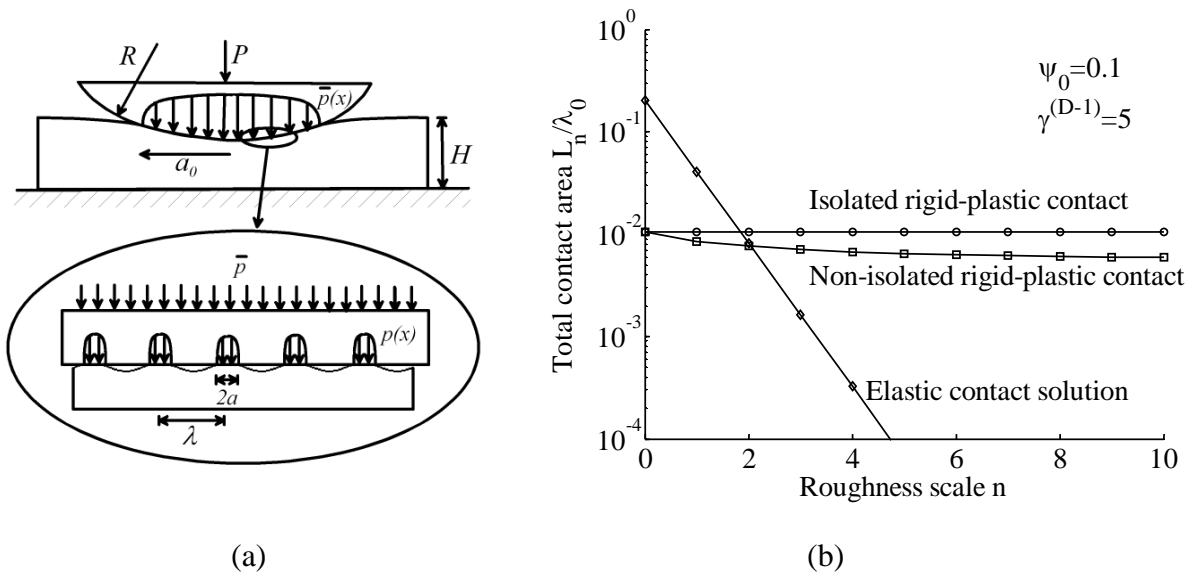


Figure 1. (a) Idealized 2D contact of a Weierstrass profile. The nominally smooth contact at the coarse scale is supported by many small asperities at the fine scale. (b) A comparison of several asymptotic solutions for fractal surface contact with $\tilde{p} = 0.1$ (see text for details).

Those asymptotic solutions can be used to extract some scaling relations for numerical simulations of self-affine fractal surface contact. The roughness spectrum is unavoidably truncated by a cutoff size, which is due to the instrument resolution in the real experimental measurement and the mesh size in the numerical calculation. The elastic contact is less sensitive to the cutoff size. By our asymptotic solution, the total true contact area is proportional to the applied load, and inversely proportional to the elastic modulus and the rms asperity slope (that scales as $\gamma^{(D-1)n}$), as also found in [6]. For the elastic-plastic contact, if the cutoff scale n_{cutoff} is sufficiently large, the true contact area will be proportional to the load by a factor of about $1/6\sigma_Y$, as also found by [7]. If the cutoff size is very coarse, or σ_Y is large, contacts at the finest asperities will deform either elastic-plastically or elastically, so that the relation between contact area and load deviates from that at low σ_Y [7]. This observation, however, critically depends on the cutoff size of mesh spacing and asperity measurement resolution. The transition between

elastic to plastic contact happens around $\lambda_{cr} \approx \lambda_0 \psi_0^{1/(D-1)}$. Thus for the elastic-plastic contact simulation, the mesh size should be less than λ_{cr} to resolve the plastic deformation field.

Properties that can be deduced from rough surface contact

The above contact analysis also suggests that contact stiffness or compliance is mainly determined by the bulk contact and the first several coarse scales. It also implies that detailed contact features at fine scales contribute insignificantly to contact properties such as thermal/electrical contact resistance, which are related to contact compliance.

Empirical relations have been established to connect the contact area and the thermal/electrical contact resistance [8]. A rigorous examination by Barber [9] proves the analogy between the conduction problem and the incremental elastic contact. Therefore, in order to predict the contact area by electrical measurements, we must refer to the relation between contact area and contact compliance. Since the contact stiffness or compliance is mainly determined by coarse scales, the electrical contact resistance is usually not affected by small asperity contacts. Consequently, the validity of determining contact area by electrical measurements is quite limited. Barber [9] also pointed out that the coarse scales give the bounds of resistance, which is confirmed by recent numerical simulations based on the elastic contact of a Weierstrass profile [10].

When the coarse scales deform plastically, those large asperities can be flattened, and the radius of curvature increases. The unloading elastic contact stiffness increases accordingly, so that the electrical contact resistance decreases.

For experiments carried out at small scales, the above argument is not justified because both continuum conduction problem and continuum plasticity are not valid. In addition, the contact compliance might be dramatically affected by the fine contact details, as will be shown by the next section.

EFFECTS OF MATERIAL LENGTH SCALES ON ROUGH SURFACE CONTACT

The above analyses and arguments are not appropriate for small scale contacts for the following reasons. The ideal fractal roughness cannot be extended to nanoscale. On the other hand, nanoscale rough surface contact is critically influenced by tribochemical effects. And it is still not clear how nanoscale asperity contacts affect the microscopic multiple asperity contacts. Mesoscale deformation mechanisms are more important. For example, using the Nix-Gao strain gradient plasticity [11] and considering the observation that smaller asperities are sharper, we derive a different scaling relation, which suggests there exists a critical wavelength below which the contact is predominately elastic [12]. The usefulness of this prediction, however, might be very limited.

The study of the micro-plasticity behavior near and at the rough surface is the critical link towards the fundamental understanding of contact, surface failures, friction and adhesion at small scales. Recently, we have developed a micromechanical dislocation model of indentation of a stepped substrate, as a unit process model [15,16]. We first consider the onset of surface yielding controlled by single-dislocation nucleation from the surface step. A dislocation can be nucleated from the stress concentration at the surface step under a combination of remote load and interface adhesion. The nucleation process can be modeled by atomistic simulations [15], which also calibrate the continuum dislocation nucleation model (Rice-Thomson model). Subsequently,

we calculate the driving force on the dislocation and construct nucleation map with respect to varying parameters such as interface adhesion, step size and lattice resistance. The nucleation and stabilization of the first dislocation from a surface step is still confined to a very small scale. We then analyze the surface hardening behavior mediated by the storage of multiple dislocations. Continuum micromechanical model of dislocation nucleation and interaction is indispensable in modeling long-range dislocation multiplication and material hardening behavior. Dislocations can be stabilized and pile up as a result of the resolved driving force and the non-zero lattice resistance in the solid. The pileup dislocations will exert a strong repulsion to further dislocation nucleation and pileup, and the subsequent increase of the applied load is needed to nucleate further dislocations, thus leading to surface hardening.

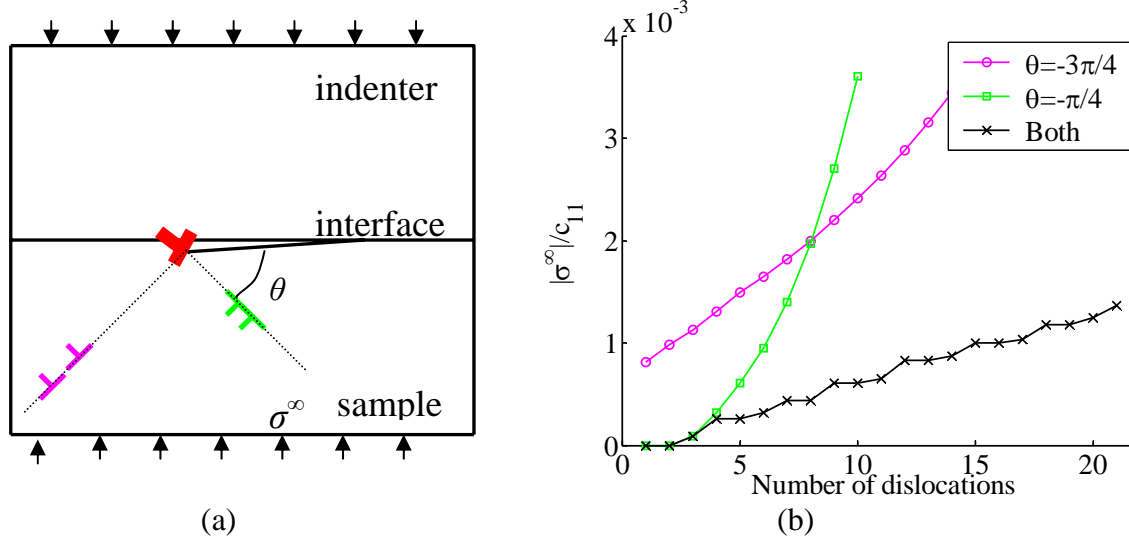


Figure 2. (a) Schematic of dislocations nucleated from a surface source (simplified by a super-dislocation). (b) The hardening curves without and with the cooperation of the two slip planes, with $h/b = 50$, $\Gamma_{adh}/c_{11}b = 0.02$, $G_p/c_{11}b = 0.001$ and $\eta/b = 5$.

Figure 2(a) shows the problem schematic. Dislocations can be nucleated from a surface source, and pile up underneath. Figure 2(b) plots the applied load against the number of nucleated dislocations. Two slip planes at $\theta = -\pi/4$ and $-3\pi/4$ are considered. The initial step height is h , and the magnitude of Burgers vector is b . The interface work of adhesion is given by Γ_{adh} , the Peierls barrier is G_p , c_{11} is one elastic constant, and η is the microstructural length used in the Rice-Thomson model. For the example shown in Fig. 2, dislocations in the right slip plane can be easily nucleated but will stay in equilibrium positions that are very close to the surface step, while dislocations in the left slip plane easily move away from the surface into the bulk. This phenomenon is called dislocation segregation. Dislocations at different slip planes segregate either close to or away from the interface, so that different slip planes, if acting separately, give rise to different degrees of surface hardening, as shown by the two smooth curves in Fig. 2(b). Amazingly, we find that the cooperation between different slip planes can make it an order-of-magnitude easier to multiply and pileup dislocations, as shown by the zig-zag curve in Fig. 2(b). This phenomenon is called latent softening. The zig-zag feature corresponds to spontaneous dislocation nucleation.

A recent molecular simulation of nanoscale asperity contact [17] shows a similar scenario, that is, dislocation nucleation, annihilation and pileup. Those works [15-17] provide some useful

insights for the nano- and meso-scale rough surface contact. In addition, adhesion is only crudely treated with a Griffith crack in Fig. 2. It is anticipated that the adhesive strength of mesoscale contact could be promoted or weakened, depending on the coupling between adhesion and micromechanics of surface plasticity. Therefore, we would have a large degree of freedom to either bond, imprint and/or peel two rough surfaces at nano- and meso-scale.

CONCLUSIONS

In this paper, we first present our contact model that is based on fractal roughness and continuum classic plasticity. Useful scaling relations can be obtained and compared with numerical simulations. However, an important conclusion from this analysis is that a perfectly fractal description of surface roughness appears to lead to unphysical predictions of the true contact size and number of contact spots, for both elastic and elastic-plastic solids. A rough surface contact model at mesoscale is still elusive, largely because of the complex behavior of dislocation plasticity. By a surface step contact model, we have examined the surface micro-plasticity, i.e. dislocation nucleation at the rough surface and the dislocation multiplication and interaction underneath. This could be the link between atomistics and bulk dislocation plasticity.

ACKNOWLEDGEMENTS

This work is supported by the Brown/General Motors Collaborative Research Lab at Brown University. The authors are grateful for discussions with Y.-T. Cheng, H.H. Yu, M.O. Robbins, M. Ciavarella and J.R. Barber. We also thank one anonymous reviewer for helpful comments.

REFERENCES

1. S. R. Forrest, *Nature* **428**, 911-918 (2004).
2. B. Bhushan, *Tribo. Lett.* **4**, 1-35 (1998).
3. K.L. Johnson, *Contact mechanics*, Cambridge Press (1985).
4. M. Ciavarella, G. Demelio, J. R. Barber and Y. H. Jang, *Proc. R. Soc. Lond. A* **456**, 387-405 (2000).
5. Y. F. Gao and A. F. Bower, submitted (2004).
6. S. Hyun, L. Pei, J.-F. Molinari and M. O. Robbins, *Phys. Rev. E* **70**, 026117 (2004).
7. L. Pei, S. Hyun, J.-F. Molinari and M. O. Robbins, submitted (2004).
8. Y. H. Jang and J. R. Barber, *J. Appl. Phys.* **94**, 7215-7221 (2003).
9. J. R. Barber, *Proc. R. Soc. Lond. A* **459**, 53-66 (2003).
10. M. Ciavarella, G. Murolo, G. Demelio and J. R. Barber, *J. Mech. Phys. Solids* **52**, 1247-1265 (2004).
11. W. D. Nix and H. Gao, *J. Mech. Phys. Solids* **46**, 411-425 (1998).
12. Y. F. Gao and A. F. Bower, unpublished work (2004).
13. A. Needleman, *Acta Mater.* **48**, 105-124 (2000).
14. I. A. Polonsky and L. M. Keer, *Proc. R. Soc. Lond. A* **452**, 2173-2194 (1996).
15. H. H. Yu, P. Shrotriya, Y. F. Gao and K.-S. Kim, unpublished work (2004).
16. Y. F. Gao, H. H. Yu and K.-S. Kim, unpublished work (2004).
17. P.-R. Cha, D. J. Srolovitz and T. K. Vanderlick, *Acta Mater.* **52**, 3983-3996 (2004).